

The Met99Gln Mutant of Amicyanin from *Paracoccus versutus*[†]

Rutger E. M. Diederix,[‡] Gerard W. Canters,^{*,‡} and Christopher Dennison^{*,§}

Gorlaeus Laboratories, Leiden Institute of Chemistry, Leiden University, Einsteinweg 55, P.O. Box 9502, 2300 RA Leiden, The Netherlands, and Department of Chemistry, University of Newcastle upon Tyne, Newcastle upon Tyne, NE1 7RU, England

Received March 21, 2000; Revised Manuscript Received May 17, 2000

ABSTRACT: The axial copper ligand methionine has been replaced by a glutamine in the cupredoxin amicyanin from *Paracoccus versutus*. Dynamic and structural characteristics of the mutant have been studied in detail using UV/Vis, EPR, NMR, cyclic voltammetry, and isomorphous metal replacement. M99Q amicyanin is a blue copper protein with significant spectral and structural similarities to the other cupredoxins umecyanin, stellacyanin, and M121Q azurin. In addition, the functional properties of M99Q amicyanin, as reflected in the electron self-exchange rate constant and midpoint potential (165 mV), have been assessed and compared to values for M121Q azurin. For the latter protein, the published midpoint potential was corrected to the much lower value of 147 mV at pH 7, $I = 0.1$ M. These values are very similar to the midpoint potential of stellacyanin, which naturally possesses an axial glutamine ligand and has the lowest reduction potential for a naturally occurring cupredoxin. A remarkable feature of M99Q amicyanin, in the reduced state, is the relatively high pK_a^* value of 7.1 for its His96 ligand.

Amicyanin from *Paracoccus versutus* (1–3) is a type 1 blue copper protein (cupredoxin) (4). These proteins have long fascinated spectroscopists because of an intense electronic (charge transfer) absorption near 600 nm, and an unusually small hyperfine coupling in the g_z region of their EPR¹ spectra (5). Moreover, their small size and single, mononuclear, redox center have facilitated numerous structural (4, 6) and electron transfer (7, 8) studies.

The copper-binding site of cupredoxins always involves three strong equatorial ligands, the N^{δ1} of two histidines and the S^γ of a cysteine, forming a copper-containing trigonal plane. A fourth, weaker, axial ligand pulls the copper out of the equatorial plane (6). In amicyanin, the coordinating

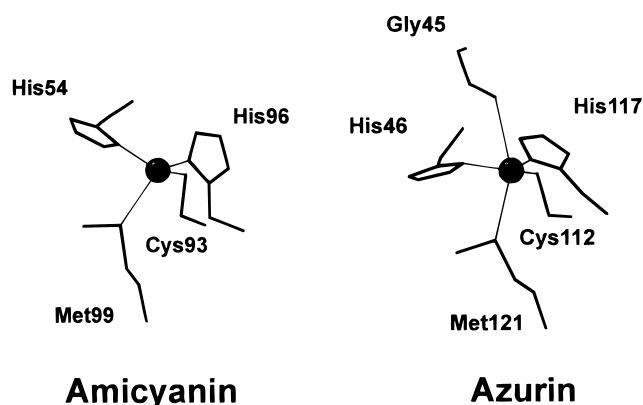


FIGURE 1: Representations of the active sites of Cu(II) amicyanin from *P. versutus* (2) and Cu(II) azurin from *A. denitrificans* (15). In both cases, the copper ion is indicated by a black sphere.

residues are His54, Cys93, His96, and Met99 (see Figure 1). In azurin, the equatorial ligands are His46, Cys112, and His117. Azurin is unique among the cupredoxins in that it possesses two weak axial ligands: the S^δ from Met121 and the backbone carbonyl oxygen of Gly45 (see Figure 1). Structural and spectroscopic work carried out to date on both native and mutant cupredoxins suggests that there is a continuum of structures, ranging from type 1 “axial” (essentially trigonal coordination plus a long bond to the axial ligand) via type 1 “rhombic” (distorted tetrahedral) and type 1.5 (tetrahedral) to type 2 (square planar) (9). In this series of structures, the axial bond is gradually shortened while the Cu–S(Cys) bond length increases. A correlation has been postulated between the length of the Cu–S(Cys) bond and the ratio between the electronic absorptions at 450 and 600 nm, and the degree of rhombicity in the EPR spectrum, properties which, likewise, reflect the strength of the axial bond. A stronger axial interaction pulls the copper out of the Cys-containing equatorial plane, both decreasing the axial

[†] This work was supported by the Foundation for Chemical Research (SON) and the Foundation for Technical Sciences (STW) with financial aid from the Netherlands Organization for Scientific Research (NWO), and under the auspices of the BIOMAC Graduate Research School of Leiden and Delft, and by a Basic Research Grant from Enterprise Ireland (to C.D.).

* Address correspondence to G.W.C. at the Department of Chemistry, University of Leiden, Gorlaeus Laboratories, P.O. Box 9502, 2300 RA Leiden, The Netherlands. Tel: +31 71 5274256, Fax: +31 71 5274349, e-mail: canters@chem.leidenuniv.nl. Address correspondence to C.D. at the Department of Chemistry, University of Newcastle upon Tyne, Newcastle upon Tyne, NE1 7RU, England. Tel: +44 191 2227127, Fax: +44 191 2226929, e-mail: christopher.dennison@ncl.ac.uk.

[‡] Leiden University.

[§] University of Newcastle-upon-Tyne.

¹ Abbreviations: UV/Vis, ultraviolet/visible; NMR, nuclear magnetic resonance; LMCT, ligand to metal charge transfer; LF, ligand field; Gdn-HCl, guanidine hydrochloride; EDTA, ethylenediaminetetraacetic acid; DTT, dithiothreitol; MES, 2-(N-morpholino)ethanesulfonic acid; HEPES, 4-(2-hydroxyethyl)piperazine-1-ethanesulfonic acid; CHES, 2-(N-cyclohexylamino)ethanesulfonic acid; DEAE, diethylaminoethyl; WEFT, water-suppressed equilibrium Fourier transform; 1D, one-dimensional; NOE, nuclear Overhauser enhancement; wt, wild type; M99Q, Met99 → Gln mutant of amicyanin; M121Q, Met121 → Gln mutant of azurin; CV, cyclic voltammetry; CBP, cucumber basic protein; EXAFS, extended X-ray absorption fine structure; EPR, electron paramagnetic resonance; NH₄Ac, ammonium acetate.

symmetry of the EPR spectrum and influencing the cysteine-to-copper charge-transfer bands, at 450 and 600 nm [as the site becomes less axial, the S(Cys) \rightarrow Cu(II) CT band at \sim 450 nm is seen to increase in intensity while that at 600 nm becomes less intense]. Solomon et al. (5) have suggested that the weakness of the axial interaction forces strong binding between the cysteine and the copper. The combined effort of the trigonal plane, holding the copper in place, and the protein matrix, keeping the axial ligand at bay, ensures that the geometrical differences between the copper site in both oxidation states is minimized. Thus, there exists a low Franck–Condon barrier, which facilitates rapid electron transfer.

Most of the cupredoxins studied to date contain a methionine as the axial ligand. An important subgroup exists in which the axial ligand is the side chain amide oxygen of a glutamine (CBP belongs to this class but possesses an axial methionine ligand) (10–13). These proteins belong to the cupredoxin subdivision called phytocyanins, which are distinguished by internal sequence homologies, an interstrand disulfide bridge, a somewhat open β -barrel structure, and relatively solvent-accessible His ligands (10–13).

Earlier work (14), concerning the replacement of the axial methionine ligand by glutamine in *Alcaligenes denitrificans* azurin, yielded an excellent spectroscopic and structural model for stellacyanin, which is the best-studied phytocyanin. In the current work, we have constructed the analogous mutant in *P. versutus* amicyanin, to study this physiologically relevant copper site interconversion in more detail. The differences between *wt* azurin and amicyanin, which highlights the need for this study, include the presence in azurin of the carbonyl oxygen of Gly45 (15), which interacts electrostatically with the copper, from an axial position, leading to a trigonal bipyramidal active site (see Figure 1). Additionally, the copper site of amicyanin is much more solvent exposed (2, 15), with the C-terminal ligand histidine protruding into the solvent. A final important difference between azurin and amicyanin is that the active site of the latter, in the reduced state, exhibits protonation of its exposed histidine ligand (16, 17), a property it shares with the plastocyanins (18, 19) and the pseudoazurins (20, 21). Protonation is known to occur at His96 of amicyanin with a pK_a^* of 6.7 (16, 22, 23). The low-pH form of Cu(I) amicyanin is therefore 3-coordinate. Consequently, the Cu(I) oxidation state is stabilized, which results in an observed increase in the redox potential (23). The dissociation of His96 also disrupts the electronic coupling pathway between the copper and external redox partners and may increase the Franck–Condon barrier for electron transfer. Thus, the electron-transfer reactivity will decrease (16). Active-site protonation has not been observed for azurin.

Currently, there is no example in the cupredoxin literature of the same mutation made in two different proteins where the structural and mechanistic consequences of the mutations have been studied in detail. We therefore have constructed the M99Q amicyanin mutant and have characterized this variant and compared the results to those obtained for the corresponding mutation in azurin (M121Q).

EXPERIMENTAL PROCEDURES

Site-Directed Mutagenesis, Protein Preparation, and Purification. Mutagenesis of Met99 to Gln was performed

using a modified version of the unique-site elimination method (24). Successful mutagenesis was confirmed by sequencing the amicyanin gene. Heterologous expression, isolation, and purification of M99Q amicyanin were performed as described earlier (3). This led to a high amount (90%) of colorless, nonoxidizable, and nonreconstitutable (with copper) amicyanin, which could not be separated from the Cu(I)-protein by ion-exchange chromatography. To improve the yield of Cu-protein, an unfolding/refolding procedure was devised, resulting in apo-protein. The unfolding/refolding procedure involved complete denaturation of the protein at pH 8.0 in 6 M Gdn-HCl, in the presence of 50 mM EDTA to chelate all divalent metal ions present, and 2 mM DTT to prevent formation of protein dimers by disulfide bridges. Refolding of apo-M99Q amicyanin was achieved by diluting the denaturation mixture rapidly 1:50 in 10 mM HEPES buffer, pH 8.0, in the presence of 5 mM DTT. For the incorporation of copper or cobalt, the protein was dialyzed against either 250 mM NH_4Ac at pH 8.0 or 10 mM MES (pH 6.5), respectively. After this step, the protein was incubated in 250 mM NH_4Ac containing 10 mM $\text{Cu}(\text{NO}_3)_2$ at pH 8.0 or in 10 mM MES containing 1 mM CoCl_2 (pH 6.5), respectively. The solution was left at room temperature for 1 h after which free metal ions were removed by dialysis. Finally, the protein was dialyzed against 10 mM HEPES at pH 8.0, and unfolded or misfolded protein was removed on a DEAE ion-exchange column at pH 7.8 (10 mM phosphate) using a linear gradient of 0–150 mM NaCl. The yield of correctly refolded, metal-reconstituted protein was approximately 60%. M121Q azurin from *A. denitrificans* was isolated as described earlier (14) and was a kind gift from Mrs. Ing. G. C. M. Warmerdam. Ultrafiltration (Amicon) with 10 kDa cutoff membranes (Millipore) was used to exchange M99Q amicyanin and M121Q azurin into various buffers and to concentrate samples.

UV/Vis Spectroscopy. Electronic spectra were recorded at 298 K (20 mM HEPES, pH 8.0) on a Shimadzu UV-2101PC UV/Vis spectrometer. The extinction coefficient of oxidized M99Q amicyanin was determined by titrating the reduced protein by $\text{K}_3[\text{Fe}(\text{CN})_6]$ and plotting the absorbance at 600 nm as a function of the added oxidant. The extinction coefficient was obtained directly from the initial slope of this plot.

EPR Spectroscopy. X-band *cw* EPR spectra were recorded on a JEOL JESRE2X spectrometer at 77 K, interfaced with an ES-PRIT330 data manipulation system. DPPH was used as the reference. The protein samples contained \sim 1 mM Cu(II) M99Q amicyanin in 40% glycerol, 10 mM HEPES at pH 8.0. The spectra were simulated as described previously (25) using a simulation program kindly provided by W. R. Hagen.

NMR Sample Preparation. For the acquisition of NMR spectra, a sample of Co(II) M99Q amicyanin was prepared in 10 mM phosphate at pH 7.0 in either 90% H_2O /10% D_2O or 99.95% D_2O , and typically contained 3–4 mM protein. The protein was exchanged into the appropriate buffer by ultrafiltration either in a stirred cell (Amicon, 5 kDa cutoff membrane) or in centrifugal ultrafiltration units (Centricon 10, Amicon). The pH values of samples were adjusted using 0.1 M NaOH or NaOD, and 0.1 M HCl or DCl as appropriate, and the pH meter readings of all D_2O solutions,

denoted as pH*, were not corrected for the deuterium isotope effect.

For the determination of the electron self-exchange rate constant, M99Q amicyanin was exchanged into deuterated 17 mM phosphate buffer at pH* 8.2 ($I = 0.05$ M). Samples were reduced by adding aliquots of 0.1 M sodium dithionite made up in 0.1 M NaOH, or using a 0.1 M sodium ascorbate solution. Fully oxidized protein was obtained using a 0.1 M solution of $K_3[Fe(CN)_6]$. The excess reductant or oxidant was removed by ultrafiltration. Reduced samples which were to be used for pH titrations were in 20 mM phosphate buffer (99.95% D_2O) and contained small amounts of sodium ascorbate to prevent reoxidation.

1H NMR Spectroscopy. 1H NMR spectra were acquired on either a Bruker WM300, a Bruker DMX600, or a Varian Unity 500 spectrometer. In some cases, 1D spectra were acquired by presaturating the H_2O or D_2O signal. One-dimensional spectra of the Cu(I) protein were also acquired using Hahn Spin–Echo (HSE) [$90^\circ - \tau - 180^\circ_y - \tau -$] ($\tau = 60$ ms) and Carr–Purcell–Meiboom–Gill (CPMG) [$90^\circ - \tau - (180^\circ_y - 2\tau)_n - 180^\circ_y - \tau$] ($n = 59$, $\tau = 1$ ms) pulse sequences. The sum of these two spectra was used to identify singlets in the aromatic region. The super-WEFT (26) sequence ($d1 - 180^\circ - \tau - 90^\circ - acq$, where $d1$ is the relaxation delay and acq is the acquisition time) was also used to suppress the D_2O signal, and also to observe fast relaxing signals in the diamagnetic region, in the spectra of Co(II) M99Q amicyanin. 1D spectra were acquired with spectral widths ranging from 10 to 600 kHz and were processed using 0–100 Hz of exponential line broadening as apodization. Steady-state 1D NOE difference spectra were acquired at two different temperatures to eliminate any chance of spectral overlap using the approach of Banci et al. (27).

WEFT-NOESY spectra were acquired using recycle times of 20–30 ms and mixing times in the range 3–10 ms. The spectral width in both dimensions was typically 50–100 kHz with 512 experiments and approximately 4096 scans per experiment. The spectra were processed into 2048×1024 data points with resolution-enhancing windows used in both dimensions.

The spin–lattice (T_1) relaxation times of the hyperfine-shifted resonances were determined using the super-WEFT sequence with a total effective relaxation delay ($d1$ plus acq) ranging from 30 to 100 ms. The interpulse delay (τ) was varied between 0.1 ms and the total effective relaxation delay. An exponential fit of the plots of peak intensity against τ , for a particular signal, yielded its T_1 value.

Self-Exchange Rate Constant Determination. For the determination of the electron self-exchange rate constant, NMR spectra were obtained of the Cu(I) protein containing various amounts of the Cu(II) species. The concentration of the Cu(II) protein present was determined by transferring the NMR sample to a 2 mm path length cuvette and measuring the absorbance at 600 nm ($\epsilon = 4200$ M $^{-1}$ cm $^{-1}$). The concentration of Cu(II) protein was determined immediately before and after the measurement of the NMR spectra, and an average of the two values was used in the calculations. The effect of increasing concentration of the oxidized protein on the line width of the resolved imidazole ring resonances of the two histidine ligands was measured. The self-exchange rate constant, k_{esc} , is obtained from the slope of plots of the exchange-induced line broadening,

ΔT_2^{-1} , against the concentration of oxidized protein (28):

$$\Delta T_2^{-1} = k_{esc} [Cu(II) \text{ M99Q amicyanin}] \quad (1)$$

Determination of Reduction Potentials. Cyclic staircase voltammetry (CV) was performed using the setup described by Hagen (29). The measurements were carried out at 298 K with a scan rate of 20 mV/s with a computer-controlled μ AUTOLAB potentiostat with GPES 4.3 software (Eco-Chemie, The Netherlands). The saturated calomel electrode was calibrated with quinhydrone (Sigma). For M99Q amicyanin, the working electrode was a flame-treated glassy carbon disk. M121Q azurin from *A. denitrificans* was measured using a gold disk working electrode, which had been cleaned (30) and modified with 4,4'-dipyridyl disulfide. The samples (~ 50 μ M) were in 100 mM phosphate, pH 7.0 ($I = 0.22$ M), except for the experiments concerning the pH dependence of the reduction potential of M121Q azurin. In the latter case, the protein was in 50 mM glycine hydrochloride, MES, HEPES, or CHES buffer ($I = 0.1$ M, NaCl), depending on pH. The potentials as measured by CV (100 mM phosphate at pH 7.0) were confirmed by the following method. Redox buffers were prepared using different ratios of $K_3[Fe(CN)_6]$ and $K_4[Fe(CN)_6]$, and $Na[Fe(EDTA)]$ and $Na_2[Fe(EDTA)]$, respectively. The redox buffers were 5 mM in concentration and in 100 mM phosphate, pH 7.0 at 298 K. Known amounts of protein were added, and the potential of the solution was measured with a saturated calomel electrode. The ratio of oxidized over reduced protein was determined optically and fitted to the Nernst equation as a function of the measured potential. Redox titrations with $K_3[Fe(CN)_6]$ failed to yield reproducible values for the midpoint potential of M99Q amicyanin, since the absorbance was not stable as a function of time at the higher degrees of oxidation. However, the initial points of the titration could be used to determine the extinction coefficient at 600 nm (vide supra).

RESULTS

Purification. The purification of M99Q amicyanin was performed according to the protocol for the *wt* protein (3). Unlike the *wt* protein, M99Q amicyanin appears to predominantly contain a colorless species (up to $\sim 90\%$) as judged from the ratio of absorption at 280 and 600 nm. Addition of solutions of $K_3[Fe(CN)_6]$ or $Cu(NO_3)_2$ does not increase the intensity of the 600 nm peak in the absorption spectrum, thus excluding the possibility that the colorless species is either reduced or apo-amicyanin. It is known from heterologously expressed azurins, in particular its M121Q variant (14), that a colorless species is co-isolated which contains Zn(II) at the active site (31, 32). Therefore, the nonblue form of M99Q amicyanin is probably Zn protein. Furthermore, unfolding and refolding of the protein in the presence of EDTA led to apo-amicyanin which could be fully reconstituted with Cu(II). This further suggests occupation of the active site by a divalent cation. It is striking that most axial methionine to glutamine mutants of cupredoxins to date, M121Q azurin (14), M92Q plastocyanin (33), and M99Q amicyanin (this study), have such a high affinity for Zn(II). In the case of plastocyanin, this results in it being very difficult to obtain copper-containing axial Met to Gln mutants (33, 34).

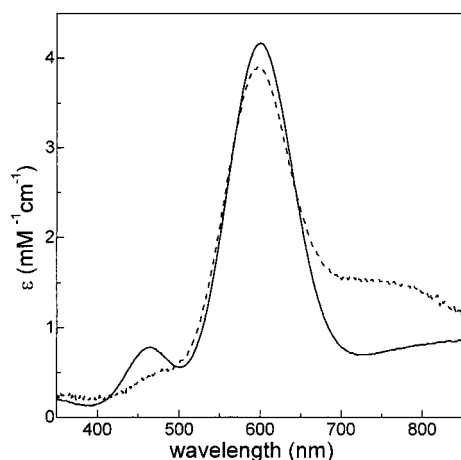


FIGURE 2: UV/Vis absorption spectra of *wt* (dashed) and M99Q (solid) amicyanin in 20 mM HEPES buffer, pH 7.0, at 298 K.

Table 1: UV/Vis Parameters of *wt* and Mutant Amicyanins and Azurins^a

<i>wt</i> amicyanin ^b	M99Q amicyanin ^c	<i>wt</i> azurin ^d	M121Q azurin ^d
460 (0.4)	465 (0.8)	460 (0.6)	452 (1.2)
596 (3.9)	600 (4.2)	619 (5.1)	610 (6.0)
750 (sh)	870 (0.9)	780 (sh)	810 (1.0)

^a Peak maxima are in nm and extinction coefficients (in parentheses) are in $\text{mM}^{-1} \text{cm}^{-1}$. ^b Reference (1). ^c This study. ^d Reference (14).

UV/Vis and EPR Spectroscopy. The UV/Vis spectrum of Cu(II) M99Q amicyanin is shown in Figure 2, together with the spectrum of *wt* amicyanin. The absorption maxima and the extinction coefficients are listed in Table 1, together with the values for *wt* and M121Q azurin from *A. denitrificans*. There is no pH dependence of the absorption spectrum of M99Q amicyanin or M121Q azurin, unlike all native phytocyanins (10, 35, 36). The absorption maxima at 596 and 460 nm (*wt*) are slightly red-shifted in the amicyanin mutant, contrary to the azurin case (see Table 1). The extinction coefficients at 465 and 600 nm have both increased with respect to the analogous bands in *wt* amicyanin, albeit not by the same factor. This results in an increase in the ratio of $\epsilon_{460}/\epsilon_{600}$ from 0.10 for *wt* to 0.18 for M99Q amicyanin. A similar increase occurred for the analogous mutation in azurin (14). This increase of the absorption ratio has been shown to be indicative of a more "rhombic" site, i.e., of a larger distance of the copper ion to the equatorial plane (37). This is supported by the EPR data, shown in Figure 3 and listed in Table 2. Simulation of the X-band EPR spectrum indicates an increase in the splitting of g_x and g_y of M99Q amicyanin as compared to *wt* amicyanin. This increase in rhombicity is smaller than in the case of the analogous mutation in azurin. A distinct feature of the EPR spectrum of M99Q amicyanin is the very small value for the hyperfine coupling A_z ($27 \times 10^{-4} \text{ cm}^{-1}$). Such a small value is usual for cupredoxins with an axial glutamine ligand (14, 38–40). In fact, when put into a Vännegård–Peisach–Blumberg plot, that is with g_z plotted against A_z , an empirical relationship transpires fitting all cupredoxins with a coordinating oxygen close together (see Figure 4).

Co(II)-Substituted M99Q Amicyanin. The UV/Vis spectra of Co(II)-substituted *wt* and M99Q amicyanin are shown in Figure 5. The main S(Cys) → Co(II) LMCT band has shifted to 314 nm in Co(II) M99Q amicyanin compared to 337 nm

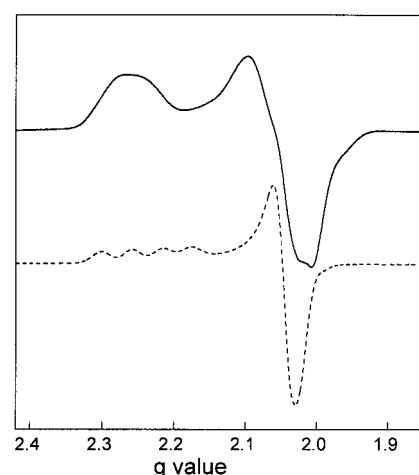


FIGURE 3: X-band EPR spectra of *wt* (dashed) and M99Q (solid) amicyanin in 20 mM HEPES buffer, pH 7.0, with 40% glycerol at 77 K.

Table 2: X-band EPR Parameters of *wt* and Mutant Amicyanins and Azurins^a

	<i>wt</i> amicyanin ^b	M99Q amicyanin ^c	<i>wt</i> azurin ^d	M121Q azurin ^e
g_x	2.033 ^f	2.030	2.039 ^g	2.028 ^h
g_y	2.050 ^f	2.052	2.057 ^g	2.083 ^h
g_z	2.239	2.270	2.258	2.287
A_z	58	27	62	35

^a A_z in $\times 10^{-4} \text{ cm}^{-1}$. ^b Reference (1). ^c This study. ^d Reference (64). ^e Reference (14). ^f From measurements at W-band [see ref (65)]. ^g From measurements at W-band [see ref (52)]. ^h From measurements at W-band [see ref (66)].

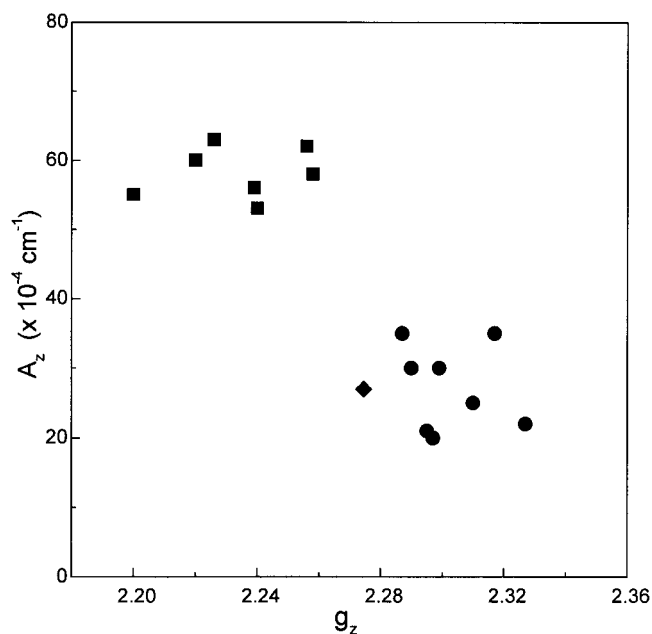


FIGURE 4: Modified Vännegård–Peisach–Blumberg plot: cupredoxins with oxygen ligation (●) and without oxygen ligation (■), including exogenous ligands (◆). M99Q amicyanin is indicated by (◆).

in the Co(II) *wt* protein. The second LMCT band has likewise undergone a blue shift, as a result of the mutation, from 389 to 367 nm. The LF transitions in the 450 to 750 nm region have also been modified in the M99Q variant but still have intensities in the range expected for Co(II) in a distorted tetrahedral environment ($\epsilon_{\text{max}} > 250 \text{ M}^{-1} \text{cm}^{-1}$).

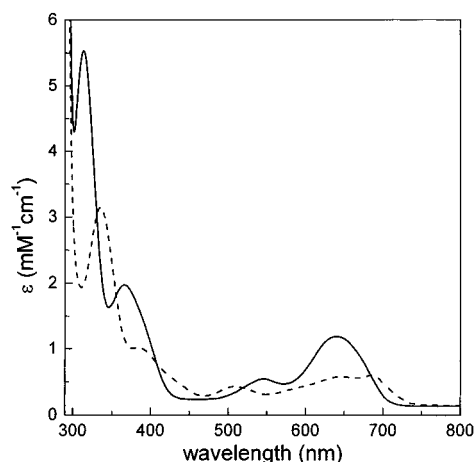


FIGURE 5: UV/Vis absorption spectra of Co(II)-substituted forms of *wt* (dashed) and M99Q (solid) amicyanin in 20 mM HEPES buffer, pH 7.0, at 298 K.

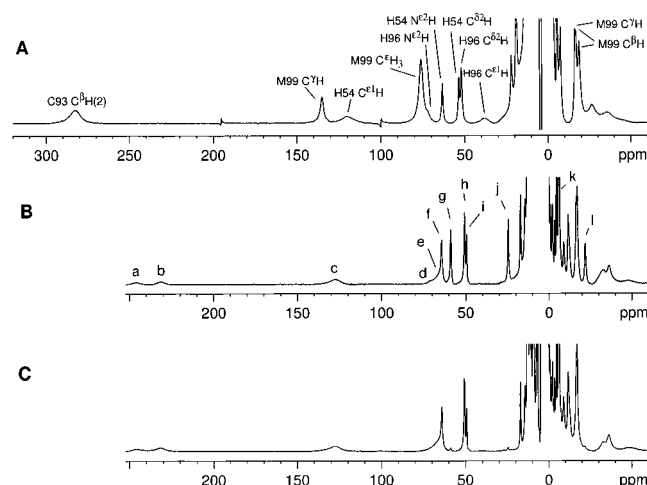


FIGURE 6: ^1H NMR spectra (300 MHz) of Co(II) *wt* amicyanin (313 K) in H_2O (pH 8.0) (A) and Co(II) M99Q amicyanin (308 K) at pH 7.0 in H_2O (B) and D_2O (C).

Assignment of the Paramagnetic ^1H NMR Spectrum of Co(II) M99Q Amicyanin. The ^1H NMR spectrum of Co(II) M99Q amicyanin is shown in Figure 6 along with the previously assigned spectrum of Co(II) *wt* amicyanin (41). The isotropically shifted resonances are listed in Table 3 along with their T_1 values and line widths. The two far-shifted broad resonances, signals a and b, in the spectrum of Co(II) M99Q amicyanin belong to the two C^βH protons of the Cys93 ligand. This is consistent with the large amount of spin density on this ligand (5, 42) and is in complete agreement with previous studies on other Co(II)-substituted cupredoxins (43, 44), and in particular those with an axial glutamine ligand (45, 46).

The spectrum of Co(II) M99Q amicyanin possesses one downfield-shifted exchangeable resonance with an intensity equivalent to one proton at pH 7.0 and 308 K (peak g, see Figure 7A). A second exchangeable resonance (peak d) increases in intensity at lower temperature (see Figure 7C). These observations are consistent with peak g belonging to the $\text{N}^{\epsilon 2}\text{H}$ proton of the buried His54 ligand, while peak d corresponds to the $\text{N}^{\epsilon 2}\text{H}$ proton of the more exposed His96 ligand (2). 1D NOE difference experiments demonstrate strong dipolar couplings between peaks g and i (Figure 7B) and peaks d and h (Figure 7D). The reverse NOEs, i.e.,

Table 3: Hyperfine-Shifted Resonances of Co(II) M99Q Amicyanin at 306 K and pH 7.0^a

resonance	δ (ppm)	T_1 (ms)	$\Delta\nu_{1/2}$ (Hz)	assignment
a	245.5	nd	1550 ^b	Cys93 C^βH
b	231.2	nd	1460 ^b	Cys93 C^βH
c	126.2	<0.5 ms	4800	His54 $\text{C}^{\epsilon 1}\text{H}$
d	77.1 ^c	nd	1135	His96 $\text{N}^{\epsilon 2}\text{H}$
e	~66	nd	nd	His96 $\text{C}^{\epsilon 1}\text{H}$
f	64.2	7.8	520	Gln99 C^γH
g	58.6	10.2	320	His54 $\text{N}^{\epsilon 2}\text{H}$
h	50.5	11.0	300	His96 $\text{C}^{\delta 2}\text{H}$
i	49.2	29.7	260	His54 $\text{C}^{\delta 2}\text{H}$
j	24.3	12.6	220	Cys93 NH
k	-6.1 ^d	nd	495 ^d	Gln99 C^γH
l	-22.1	5.6	420	Gln99 $\text{N}^{\epsilon 2}\text{H}$

^a Data recorded at 500 MHz. Also included are the spin-lattice (T_1) relaxation times, the chemical shifts, the peak widths ($\Delta\nu_{1/2}$), and the assignments that have been made. ^b Measured at 300 MHz. ^c This resonance was observed at 278 K and 600 MHz. ^d Measured from a 1D NOE experiment at 600 MHz.

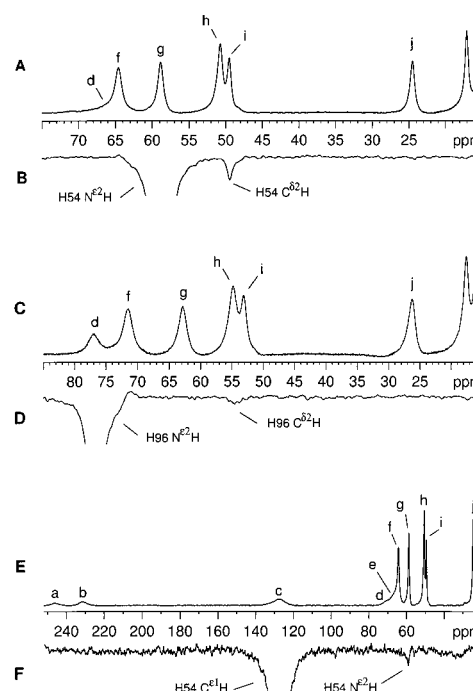


FIGURE 7: Reference (A, C, and E) and difference (B, D, and F) spectra corresponding to 1D NOE experiments performed in H_2O (pH 7.0) on Co(II) M99Q amicyanin. Spectra A–D were recorded at 600 MHz, and at 308 K for spectra A and B and at 278 K for spectra C and D. Spectra E and F were recorded at 300 MHz and at 308 K.

between peaks i and g and also between peaks h and d, were also observed (data not shown). The small line width of peaks i and h and their relatively long T_1 relaxation times indicate that these protons are not within 4 Å of the metal ion, and therefore must belong to the $\text{C}^{\delta 2}\text{H}$ resonances of His54 and His96, respectively (this is the expected pattern when the histidine coordinates via its N^{δ} atom). The very broad resonance c, upon irradiation, shows an NOE to signal g (Figure 7F). This clearly identifies resonance c as the $\text{C}^{\epsilon 1}\text{H}$ of the imidazole ring of His54 because this proton is much closer to the metal ion, hence its much broader nature and shorter T_1 value. The second, very broad signal in this region of the spectrum, peak e, can therefore be assigned to the $\text{C}^{\epsilon 1}\text{H}$ of His96.

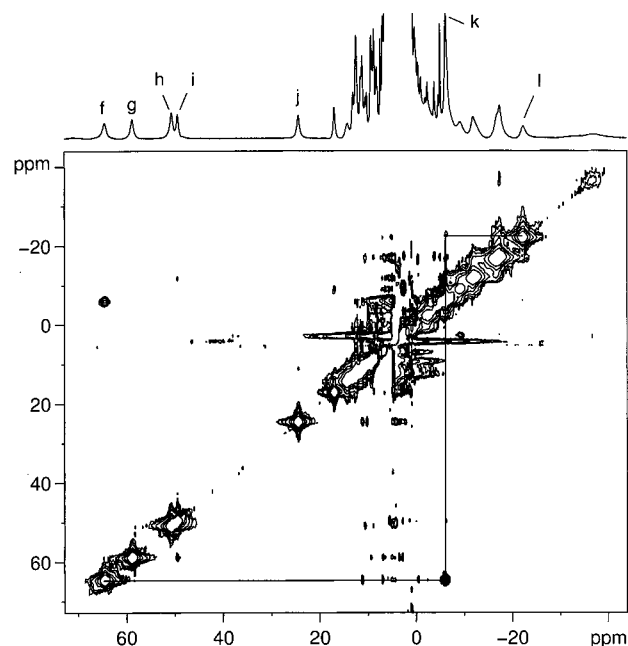


FIGURE 8: Part of the WEFT-NOESY spectrum of Co(II) M99Q amicyanin in H₂O at 308 K with a mixing time of 5 ms.

In the WEFT-NOESY spectrum shown in Figure 8, peak f shows a strong NOE to signal k, which is made up of at least two overlapping resonances. This strong NOE is consistent with a geminal pair of protons. Peak f, in a 1D NOE difference experiment, also shows a weak NOE to the exchangeable resonance l (data not shown). An NOE is clearly observed between peaks k and l in the NOESY spectrum (Figure 8). All of these observations, along with similar studies carried out on other cupredoxins with an axial glutamine ligand (45, 46), clearly point to these three resonances belonging to the axial glutamine ligand with peaks f and k being the C^αH protons and peak l belonging to one of the N^εH protons.

Finally, the exchangeable signal j can be tentatively assigned as the NH of Cys93. This conclusion is based upon the observation of an NOE between one of the C^βH resonances of Cys93 (peak b) and peak j in a 1D NOE difference experiment in which resonance b was irradiated (data not shown).

Reduction Potentials. M121Q azurin yielded good, quasi-reversible responses on a 4,4'-dipyridyl disulfide-modified gold electrode. The anodic and cathodic peaks were of equal intensity, and their separation was approximately 60 mV at a scan rate of 20 mV/s. The peak currents were proportional with the (scan rate)^{1/2}. The midpoint potential of M121Q azurin showed a gradual increase from pH 9.0 to pH 4.5 with a slope of ~10 mV/pH unit (see Figure 9). At pH 7.0, a value of 147 mV for the midpoint potential of M121Q azurin (see Table 4) was found. This value is quite different from that reported previously (263 mV; see ref 14) from a redox titration of this protein with the [Fe(CN)₆]^{3-/4-} couple (410 mV). The erroneous nature of this value must be due to the large difference between the potential of the metal complex used and that of the protein. Because of this large discrepancy, the midpoint potential of M121Q azurin was also determined by an alternative method. In this, the ratio of oxidized to reduced protein was determined as a function of the solution potential, and the CV data could be confirmed

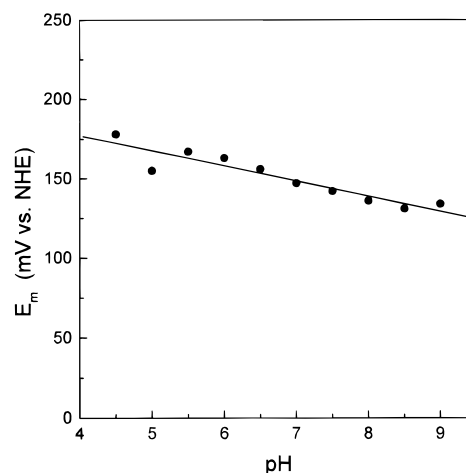


FIGURE 9: Reduction potential of M121Q azurin as a function of pH (●), as measured by CV (see Experimental Procedures). A linear fit (slope 9.5 ± 2 mV/pH unit) is shown as a solid line.

Table 4: Redox Potentials of wt and Mutant Amicyanins and Azurins^a

	wt amicyanin	M99Q amicyanin	wt azurin	M121Q azurin
CV	250 ± 3 ^b	165 ± 5 ^d	268 ± 2 ^e	147 ± 5 ^d
titration	260 ± 2 ^c	165 ± 30 ^d	286 ± 4 ^e	136 ± 25 ^d

^a Values in mV vsNHE; all values quoted were obtained at pH 7.0.

^b Reference (23). ^c Reference (1). ^d This study. ^e Reference (67).

(see Table 4). For M99Q amicyanin, the CV response was not ideal. Although the response was quasi-reversible, as judged from the scan rate dependence of the peak currents, the anodic and cathodic peaks were never of equal area and amplitude. Nevertheless, the value estimated from CV at pH 7.0 (165 mV) fits nicely with that obtained by the alternative method described above (see Table 4).

pK_a of His96 Determined by ¹H NMR. The histidine resonances of Cu(I) M99Q amicyanin were identified by examination of the singlets in the aromatic region (6.0–8.5 ppm) of the spectrum (see Experimental Procedures). A pH-dependent displacement of two singlets in this region was observed. By analogy to wt amicyanin, the singlets were assigned to the C^εH and C^δ2H protons of His96 with their pH dependence being due to the protonation of the N^δ1 of His96, and with the C^εH proton assigned on the basis of its greater sensitivity to pH (47). The chemical shift of these two singlets, especially of the C^εH resonance, could be followed during the entire titration, down to pH* 5.6, where detection was impossible due to severe broadening of the signal [analogous to the situation found for wt amicyanin (16)]. The pH dependence of the chemical shift of the C^εH proton of His96 is shown in Figure 10. The pK_a* of His96 was determined from the chemical shift data using the equation:

$$\delta = (K_a \delta_H + [H^+] \delta_L) / (K_a + [H^+]) \quad (2)$$

where δ_H and δ_L are the chemical shifts at high and low pH, respectively. A three-parameter nonlinear least-squares fit of the data yielded a pK_a* of 7.1 for the N^δ1 of His96 in Cu(I) M99Q amicyanin.

Electron Self-Exchange Rate Constant Determination. The electron-transfer reactivity of M99Q amicyanin was exam-

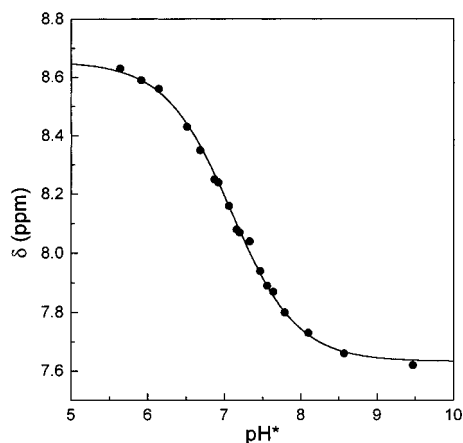


FIGURE 10: Position of the His96 C ϵ 1 proton resonance of M99Q amicyanin as a function of pH* (●). The solid line is the result of a simulation using eq 2.

ined by measuring the electron self-exchange (ese) rate constant using ^1H NMR spectroscopy. The measurements were performed at pH* 8.2, well above the $\text{p}K_{\text{a}}^*$ of His96 (vide supra) and thus where the pH dependence of the reactivity is expected to be minimal. An ese rate constant of $1.1 \times 10^4 \text{ M}^{-1} \text{ s}^{-1}$ was determined for M99Q amicyanin, which is approximately 12-fold smaller than the value of $1.3 \times 10^5 \text{ M}^{-1} \text{ s}^{-1}$ found for *wt* amicyanin under identical conditions (16).

DISCUSSION

UV/Vis Spectrum of Co(II) Amicyanin. The electronic spectrum of Co(II) M99Q amicyanin is consistent with a tetrahedral Co(II) site ($\text{LF } \epsilon_{\text{max}} > 250 \text{ M}^{-1} \text{ cm}^{-1}$, vide supra). A blue shift of the main S(Cys) \rightarrow Co(II) LMCT band is observed in the UV/Vis spectrum of Co(II) M99Q amicyanin when compared to Co(II) *wt* amicyanin. A similar effect has also been observed in Co(II) azurin upon making the M121E (48) and M121Q (45) mutations. In the case of the former variant, the oxygen atom of a carboxylate group coordinates the metal ion in the axial position. This results in the observed blue shifts being much greater due to the enhanced polarity of the carboxylate side chain. The optical spectrum therefore shows that in Co(II) M99Q amicyanin the coordination of the introduced glutamine most probably occurs via its side chain carbonyl oxygen. The spectrum of Co(II) M99Q amicyanin is also very similar to that of Co(II) stellacyanin (49), further supporting coordination via the side chain oxygen of the glutamine (11, 14), and is also reminiscent of the spectrum of Co(II) mavicyanin (50).

The Paramagnetic ^1H NMR Spectrum of Co(II) M99Q Amicyanin. The assigned paramagnetic ^1H NMR spectrum of Co(II) M99Q amicyanin (Figure 6 and Table 3) provides detailed structural information about the metal binding site of this protein. Most importantly, the observation of one of the N ϵ H protons of Gln99 clearly demonstrates that the introduced axial ligand coordinates to Co(II) via its side chain carbonyl oxygen. Coordination by the deprotonated side chain amide nitrogen would result in the remaining proton on this atom being extremely close to the metal ion and its resonance being very broad and having a much shorter T_1 relaxation time than peak 1 possesses.

Table 5 lists the hyperfine shifts of the assigned peaks of Co(II) M99Q amicyanin along with the analogous signals

in Co(II) *wt* amicyanin. Also included are the shifts of the corresponding resonances in Co(II) *wt* azurin, Co(II) M121Q azurin, and Co(II) stellacyanin. In the case of Co(II) azurin [from *Pseudomonas aeruginosa* which has a paramagnetic ^1H NMR spectrum for the Co(II) protein almost identical to that of the *A. denitrificans* protein], the orientation of the magnetic susceptibility (χ) tensor has been determined. This has allowed the Fermi-contact contribution to the isotropic shifts of protons on the ligating residues to be resolved from their pseudo-contact (dipolar) part (51). The orientation of the χ -tensor results in the isotropic shifts of the C $^\beta$ H resonances of the cysteine ligand being mainly Fermi-contact in origin. Additionally, the shift of the C $^\gamma$ H proton of the axial Met ligand is composed mainly of a Fermi-contact contribution, whereas the shift of the C $^\gamma$ H proton of this residue is mainly dipolar in origin. The orientation of the χ -tensor is very similar in *wt* azurin and in the M121Q azurin mutant (52). This is especially so when you consider the z -axis of the tensor, and so the pattern of dipolar and Fermi-contact contributions to the isotropic shifts of protons on the axial ligand will also hold when a glutamine ligand is present at the active site of a cupredoxin (45, 46, 51). It should be remembered, however, when making comparisons between cupredoxins possessing axial Met and Gln ligands, that the Gln C $^\gamma$ H protons are four bonds from the metal ion whereas the Met C $^\gamma$ H protons are only three bonds away.

An interesting feature of the ^1H NMR spectrum of Co(II) M99Q amicyanin is the shift of the Cys93 C $^\beta$ H protons. In Co(II) *wt* amicyanin, these two resonances are thought to overlap at 285 ppm (Table 5). In the M99Q mutant, the two protons are resolved by ~ 16 ppm, and their shifts are considerably smaller. The resolution of the Cys C $^\beta$ H resonances in Co(II) M99Q amicyanin indicates slight differences in the Co(II)–S $^\gamma$ –C $^\beta$ –H $^\beta$ dihedral angles, a modified orientation of the magnetic susceptibility tensor, or a combination of these two effects as compared to Co(II) *wt* amicyanin. The reduced shift of the Cys C $^\beta$ H resonances provides indirect evidence of a stronger axial interaction at the active site of M99Q amicyanin as compared to the *wt* protein as well as indicating a weaker Co(II)–S(Cys) bond in the former.

When compared to other cupredoxins which possess an axial glutamine ligand, the isotropic shifts observed for the Cys C $^\beta$ H protons appear to be larger in M99Q amicyanin (see Table 5). This suggests that the Cu–S bond is relatively stronger in M99Q amicyanin versus the other glutamine-ligating cupredoxins. A similar conclusion is also drawn from comparisons of the isotropic shifts of these cysteinyl resonances in *wt* amicyanin as compared to other Co(II)-substituted cupredoxins with an axial methionine ligand (41).

The isotropic shifts of the C $^\gamma$ H protons of the axial glutamine ligand in Co(II) M99Q amicyanin are very similar to those observed for Co(II) M121Q azurin and Co(II) stellacyanin. The shift of the observed N ϵ H signal of Co(II) M99Q amicyanin and M121Q azurin is also very similar [the corresponding resonance was not observed in Co(II) stellacyanin]. All of this information points to very similar modes of coordination of the axial glutamine ligand in these three proteins, with the homology between Co(II) M99Q amicyanin and Co(II) stellacyanin being greatest (see Table 5). Considering that the shift of the C $^\gamma$ H protons of the axial glutamine ligand is mainly contact in origin, it is perhaps

Table 5: Observed Hyperfine Shifts in ppm in the ^1H HMR Spectrum of Co(II) M99Q Amicyanin Compared with the Corresponding Values for Co(II) *wt* Amicyanin (41)^a

ligand ^b	proton	Co(II) <i>wt</i> amicyanin	Co(II) M99Q amicyanin	Co(II) <i>wt</i> azurin	Co(II) M121Q azurin	Co(II) stellacyanin
His	C ^{δ2} H	52.6	49.2	48.9	47.2	45.3
	C ^{ϵ1} H	117.5/37.8 ^c	126.2	76/90 ^c	83/125 ^c	115
	N ^{ϵ2} H	62.5	58.6	75.6	73.4	74.4
Cys	C ^{β} H ₂	285	231/245 ^d	222/262 ^d	183/224 ^d	180/206 ^d
His	C ^{δ2} H	51.0	50.5	56.7	56.8	51.4
	C ^{ϵ1} H	117.5/37.8 ^c	~66	76/90 ^c	83/125 ^c	86
	N ^{ϵ2} H	74.0	77.1	64.4	67.4	63.4
Met	C ^{γ1} H	130.7		39.2		
	C ^{γ2} H	10.0		-14.7		
	C ^{ϵ} H ₃	74.5		-5.7		
Gln	C ^{γ1} H		64.2		46.4	66.2
	C ^{γ2} H		-6.1		-12.8	-5.8
	N ^{ϵ2} H		-22.1		-26.4	
Gly	C ^{α1} H			49.0	5.9	
	C ^{α2} H			-26.3	-10.5	

^a Also included in the comparison are the values for Co(II) *wt* azurin (45), M121Q Co(II) azurin (45), and stellacyanin (46). ^b From top to bottom, His54, Cys93, His96, and Met99 for *wt* amicyanin; His54, Cys93, His96, and Gln99 for M99Q amicyanin; His46, Cys112, His117, Met121, and Gly45 for *wt* azurin; His46, Cys112, His117, and Gln121 for M121Q azurin; His46, Cys87, His92, and Gln97 for stellacyanin. ^c These resonances have not been assigned to a particular His. ^d Stereospecific assignments have not been made.

interesting to speculate that the strength of the axial bond in Co(II) stellacyanin and Co(II) M99Q amicyanin is almost identical, and slightly greater than that in Co(II) M121Q azurin. This difference in bond strength might also be reflected in the slightly larger metal Cu—O(Gln) distance observed in the crystal structure of stellacyanin compared to M121Q azurin (11, 14). Another interesting aspect of this study is the effect the Met \rightarrow Gln mutation has on the shifts of the C ^{γ} H resonances of the axial ligand in amicyanin and azurin. In the *wt* proteins, the Co(II)—S(Met) interaction is much stronger in amicyanin due to the absence of a second axially interacting ligand in this protein (41). It seems that the strength of the original Co(II)—S(Met) bond of the *wt* protein is of no consequence, and both the azurin and amicyanin variants have a very similar active site.

The shift pattern of the protons on the two histidine ligands is remarkably similar in all of the glutamine-ligating cupredoxins (see Table 5). For the C ^{δ 2}H and the N ^{ϵ 2}H resonances, the contact contribution dominates (51), so the comparable chemical shift values are an indication of very similar coordination of the histidines in these proteins. The His C ^{ϵ 1}H protons, which are close to the paramagnetic center and experience large pseudo-contact shifts, also exhibit similar shift patterns in the three proteins which have axial glutamine ligands. This not only supports the similar coordination mode of the histidine ligands, but also confirms the very similar orientation of the magnetic susceptibility tensor in these proteins.

Spectroscopy and Redox Properties of the Cu Site. The previous section demonstrates that the metal sites of Co(II)-substituted M99Q amicyanin and M121Q azurin are exceedingly similar. Spectroscopic and electrochemical studies indicate that the Cu(II) proteins also have very comparable active sites. The data in Tables 1 and 2 show that the electronic structure of the Cu(II) site is very similar in both proteins, and that it is very similar to the spectroscopy of the glutamine-ligand-containing phytocyanins (14, 38–40). The copper site is type 1 rhombic, and the axial ligand is the carbonyl oxygen of the glutamine side chain. The mutation of the axial Met to Gln has caused almost exactly

the same spectral changes in the Cu(II) forms of amicyanin and azurin, despite the structural difference at the active sites of both *wt* proteins.

The resemblance of the effect of the mutation in both proteins is also reflected in the electrochemistry of the mutants. We have determined the redox potential of M99Q amicyanin and M121Q azurin by two independent methods. In contrast to the value erroneously reported earlier (14), M121Q azurin has a much lower redox potential than *wt* azurin. This large decrease in potential versus the parental *wt* protein (1) is also observed for M99Q amicyanin (Table 4). It is not surprising that the introduction of Gln has the effect to lower the redox potential, and this has been anticipated by many researchers to date (14, 53). This is also in line with the reduction potential of stellacyanin (54, 55). It is thought that the introduced oxygen ligand has a preference for Cu(II) over Cu(I) and thus leads to the lowering of the reduction potential. What is striking, is that the effect of the mutation on the potential is about equally large (lowered by roughly 100 mV) for both amicyanin and azurin, despite the structural differences between both *wt* proteins. In addition, a comparable decrease in the reduction potential was observed in a number of other Met \rightarrow Gln mutated type 1 copper sites (rusticyanin, plastocyanin, and bilirubin oxidase) (33, 56, 57) and a comparable increase was observed for the opposite, Gln \rightarrow Met mutation in a number of phytocyanins (58, 59). This indicates that in general, substituting the axial methionine by glutamine or vice versa has a limited influence on the reduction potential of the blue copper site, namely, 35–160 mV (33, 56–59). A similar limited effect on the reduction potential has been observed in cases where other amino acids are involved in axial ligation (60–62). Considering the large range of reduction potentials encompassed by type 1 sites, the nature of the axial ligand cannot be the only factor in controlling this parameter. Clearly other features such as the orientation of protein dipoles around the copper site and variations in the solvent accessibility of the metal ion are important.

The reactivity in terms of the electron self-exchange rate constant has been measured for M99Q amicyanin. It amounts

to $1.1 \times 10^4 \text{ M}^{-1} \text{ s}^{-1}$, vs $1.3 \times 10^5 \text{ M}^{-1} \text{ s}^{-1}$ for *wt* amicyanin under identical conditions (16). The rate constant in the mutant protein is still fairly high, and M99Q amicyanin is a perfectly redox-active protein. The small drop in the *ese* rate constant (12-fold) suggests that the integrity of the Cu site in this protein is still intact in both oxidation states. In M121Q azurin, the drop in the *ese* rate constant caused by the mutation is somewhat larger, ~63-fold (14). In the latter case, the drop in rate was attributed fully to a considerable conformational change that occurs upon reduction; the Cu adopts an almost linear coordination between Cys112 and His46 (14). The decrease in *ese* for the amicyanin mutant is not so severe, thus suggesting that conformational changes at the active site of M99Q amicyanin upon reduction or oxidation at pH 8 are somewhat smaller than in the case of M121Q azurin (but *vide infra*).

In the case of three different cupredoxins, plastocyanin, amicyanin, and pseudoazurin, it is clearly established that in the reduced protein the C-terminal histidine ligand protonates (16–21). This has been suggested to correspond with the relatively small number of residues separating the coordinating residues in the ligand-bearing loop (20), but recent loop-directed mutagenesis studies on amicyanin have shown that this is too simple a concept (63). While the pK_a of the His is already high in *wt* amicyanin, pK_a^* 6.7 (16), in M99Q amicyanin it is even higher (pK_a^* 7.1). The reason for the high pK_a in *wt* amicyanin is not completely understood at present. One possibility is that the more exposed nature of the active site in this protein may be significant. We do not think that the increase in pK_a in the M99Q variant is the result of a grossly different structure around the metal center (14). It seems more likely that the origin of the higher pK_a is due to a weakening of the metal–His bond in the mutant with respect to *wt* amicyanin. Thus, analogous to M121Q azurin, the Gln in M99Q amicyanin has the property to weaken the bond between the C-terminal His and Cu(I) relative to the *wt* proteins. It is interesting to observe that in the reduced *wt* azurins the C-terminal histidine has been found not to titrate with pH. As judged from the small variation of the redox potential with pH (see Figure 9), this property appears to be conserved in the M121Q azurin variant. The observed small and gradual change of the redox potential with pH can be fully explained by invoking a gradual change in the overall charge of the M121Q azurin with pH.

CONCLUSIONS

The paramagnetic ^1H NMR studies on Co(II) M99Q amicyanin demonstrate that the active site of this protein is very similar to those of Co(II) M121Q azurin and Co(II) stellacyanin. Interestingly, even though the Co(II)–O(Gln) interactions are very similar in these three proteins, the Co(II)–S(Cys) bond is stronger in M99Q amicyanin. Another interesting conclusion from this part of the study is that in both amicyanin and azurin, which have distinct differences in the strength of the bonds to the axial ligands at their active sites (2, 15, 40), the axial Met \rightarrow Gln mutation results in variants with very similar axial Co(II)–O(Gln) bonds.

The spectroscopic and mechanistic studies on the copper proteins demonstrate that M99Q amicyanin and M121Q azurin are comparable. This similarity implies that the effect

that the introduced glutamine has on the copper site is not related to the starting structures in which the axial ligand is replaced. The more important effect is the interaction of the copper with the introduced oxygen. Thus, even though in *wt* azurin the interaction of Cu(II) with Gly45 leads to an increase in the Cu–S(Met) distance as compared to *wt* amicyanin (3.11 vs 2.84 Å), this effect is not translated to the Met \rightarrow Gln mutants. This conclusion is also supported by the spectroscopic similarities between these two mutants and the phytocyanins which possess an axial glutamine ligand. In the reduced form, both mutants appear to display a weakened His–Cu bond with respect to their parental *wt* proteins. It remains to be determined whether in this respect these mutants are good models for Cu(I) phytocyanins. In other words, whether all cupredoxins containing an axial glutamine ligand, including the phytocyanins, are characterized by a labile Cu–His bond.

ACKNOWLEDGMENT

Dr. Jesús Salgado is gratefully acknowledged for helpful discussions.

REFERENCES

1. van Houwelingen, T., Canters, G. W., Stobbelaar, G., Duine, J. A., Frank, J., and Tsugita, A. (1985) *Eur. J. Biochem.* **153**, 75–80.
2. Romero, A., Nar, H., Huber, R., Messerschmidt, A., Kalverda, A. P., Canters, G. W., Durely, R., and Mathews, F. S. (1994) *J. Mol. Biol.* **236**, 1196–1211.
3. Kalverda, A. P., Wymenga, S. S., Lommen, A., van de Ven, F. J. M., Hilbers, C. W., and Canters, G. W. (1994) *J. Mol. Biol.* **240**, 358–371.
4. Adman, E. T. (1985) in *Topics in Molecular and Structural Biology: Metalloproteins* (Harrison, P. M., Ed.) Vol. 6, Part 1, pp 1–42, Verlag Chemie, Weinheim.
5. Solomon, E. I., Penfield, K. W., Gewirth, A. A., Lowery, M. D., Shadle, S. E., Guckert, J. A., and LaCroix, L. B. (1996) *Inorg. Chim. Acta* **243**, 67–78.
6. Adman, E. T. (1991) *Adv. Protein Chem.* **42**, 144–197.
7. Farver, O., and Pecht, I. (1994) in *Copper Proteins and Copper Enzymes* (Lontie, R., Ed.) Vol. 1, pp 183–214, CRC, Boca Raton, FL.
8. Farver, O. (1996) in *Protein Electron Transfer* (Bendall, D. S., Ed.) pp 161–188, Bios, Oxford, U.K.
9. Andrew, C. R., Yeom, H., Valentine, J. S., Karlsson, B. G., Bonander, N., van Pouderoyen, G., Canters, G. W., Loehr, T. M., and Sanders-Loehr, J. (1994) *J. Am. Chem. Soc.* **116**, 11489–11498.
10. van Driessche, G., Dennison, C., Sykes, A. G., and van Beeumen, J. (1995) *Protein Sci.* **4**, 209–227.
11. Hart, P. J., Nersissian, A. M., Herrmann, R. G., Nalbandyan, R. M., Valentine, J. S., and Eisenberg, D. E. (1996) *Protein Sci.* **5**, 2175–2183.
12. Nersissian, A. M., Mehrabian, Z. B., Nalbandyan, R. M., Hart, P. J., Fraczekiewicz, G., Czernuszewicz, R. S., Bender, C. J., Peisach, J., Herrmann, R. G., and Valentine, J. S. (1996) *Protein Sci.* **5**, 2184–2192.
13. Guss, J. M., Meritt, E. A., Phizackerley, R. P., and Freeman, H. C. (1996) *J. Mol. Biol.* **262**, 686–705.
14. Romero, A., Hoitink, C. W. G., Nar, H., Huber, R., Messerschmidt, A., and Canters, G. W. (1993) *J. Mol. Biol.* **229**, 1007–1021.
15. Baker, E. N. (1988) *J. Mol. Biol.* **203**, 1071–1095.
16. Lommen, A., and Canters, G. W. (1990) *J. Biol. Chem.* **265**, 2768–2774.
17. Lommen, A., Pandya, K. I., Koningsberger, D. C., and Canters, G. W. (1991) *Biochim. Biophys. Acta* **1076**, 439–447.
18. Segal, M. G., and Sykes, A. G. (1978) *J. Am. Chem. Soc.* **100**, 4585–4592.

19. Guss, J. M., Harrowell, P. R., Murata, M., Norris, V. A., and Freeman, H. C. (1986) *J. Mol. Biol.* 192, 361–387.
20. Dennison, C., Kohzuma, T., McFarlane, W., Suzuki, S., and Sykes, A. G. (1994) *Inorg. Chem.* 33, 3299–3305.
21. Vakoufari, E., Wilson, K. S., and Petratos, K. (1994) *FEBS Lett.* 347, 203–206.
22. Lommen, A., Wijmenga, S., Hilbers, C. W., and Canters, G. W. (1991) *Eur. J. Biochem.* 201, 695–702.
23. Dennison, C., Vijgenboom, E., Hagen, W. R., and Canters, G. W. (1996) *J. Am. Chem. Soc.* 118, 7406–7407.
24. Deng, W. P., and Nickoloff, J. A. (1992) *Anal. Biochem.* 260, 81–88.
25. van Pouderoyen, G., den Blaauwen, T., Reedijk, J., and Canters, G. W. (1996) *Biochemistry* 35, 13205–13211.
26. Inubushi, T., and Becker, E. D. (1983) *J. Magn. Reson.* 51, 128–133.
27. Banci, L., Bertini, I., Luchinat, C., Piccioli, M., Scozzafava, A., and Turano, P. (1989) *Inorg. Chem.* 28, 4650–4656.
28. Groeneveld, C. M., and Canters, G. W. (1988) *J. Biol. Chem.* 263, 167–173.
29. Hagen, W. R. (1989) *Eur. J. Biochem.* 182, 523–530.
30. Katz, E., Schlereth, D. D., and Schmidt, H. L. (1994) *J. Electroanal. Chem.* 367, 59–70.
31. van de Kamp, M., Hali, F. C., Rosato, N., Finazzi-Agro, A., and Canters, G. W. (1990) *Biochim. Biophys. Acta* 1019, 283–292.
32. Nar, H., Huber, R., Messerschmidt, A., Filipou, A. C., Barth, M., Jaquinod, M., van de Kamp, M., and Canters, G. W. (1992) *Eur. J. Biochem.* 205, 1123–1129.
33. Hibino, T., Lee, B. H., Takabe, T., and Takabe, T. (1995) *J. Biochem. (Tokyo)* 117, 101–106.
34. Chang, T. K., Iverson, S. A., Rodrigues, C. G., Kiser, C. N., Lew, A. Y. C., Germanas, J. P., and Richards, J. H. (1991) *Proc. Natl. Acad. Sci. U.S.A.* 88, 1325–1329.
35. Peisach, J., Levine, W. G., and Blumberg, W. E. (1967) *J. Biol. Chem.* 242, 2847–2858.
36. Fernández, C. O., Sannazzaro, A. I., and Vila, A. J. (1997) *Biochemistry* 36, 10566–10570.
37. Lu, Y., Roe, J. A., Gralla, E. B., and Valentine, J. S. (1993) in *Bioinorganic chemistry of copper* (Karlin, K. D., and Tyeklár, Z., Eds.) pp 64–77, Chapman & Hall, New York.
38. Malmström, B. G., Reinhammar, B., and Vänngård, T. (1970) *Biochim. Biophys. Acta* 205, 48–57.
39. Stigbrand, T., Malmström, B. G., and Vänngård, T. (1971) *FEBS Lett.* 12, 260–262.
40. Marchesini, A., Minelli, M., Merble, H., and Kroneck, P. M. H. (1979) *Eur. J. Biochem.* 101, 77–84.
41. Salgado, J., Kalverda, A. P., Diederix, R. E. M., Canters, G. W., Moratal, J. M., Lawler, A. T., and Dennison, C. (1999) *J. Biol. Inorg. Chem.* 4, 457–467.
42. Bertini, I., Ciurli, S., Dikiy, A., Gasanov, R., Luchinat, C., Martini, G., and Safarov, N. (1999) *J. Am. Chem. Soc.* 121, 2037–2046.
43. Salgado, J., Jiménez, H. R., Donaire, A., and Moratal, J. M. (1995) *Eur. J. Biochem.* 231, 358–369.
44. Piccioli, M., Luchinat, C., Mizoguchi, T., Ramirez, B. E., Gray, H. B., and Richards, J. H. (1995) *Inorg. Chem.* 34, 737–742.
45. Salgado, J., Jiménez, H. R., Moratal, J. M., Kroes, S., Warmerdam, G. C. M., and Canters, G. W. (1996) *Biochemistry* 35, 1810–1819.
46. Vila, A. J., and Fernández, C. O. (1996) *J. Am. Chem. Soc.* 118, 7291–7298.
47. Lommen, A., Canters, G. W., and van Beeumen, J. (1988) *Eur. J. Biochem.* 176, 213–223.
48. DiBilio, A. J., Chang, T. K., Malmström, B. G., Gray, H. B., Karlsson, B. G., Nordling, M., Pascher, T., and Lundberg, L. G. (1992) *Inorg. Chim. Acta* 198–200, 145–148.
49. McMillin, D. R., Rosenberg, R. C., and Gray, H. B. (1974) *Proc. Natl. Acad. Sci. U.S.A.* 71, 4760–4762.
50. Maritano, S., Marchesini, A., and Suzuki, S. (1997) *J. Biol. Inorg. Chem.* 2, 177–181.
51. Donaire, A., Salgado, J., and Moratal, J. M. (1998) *Biochemistry* 37, 8659–8673.
52. Coremans, J. W. A., Poluektov, O. G., Groenen, E. J. J., Canters, G. W., Nar, H., and Messerschmidt, A. (1994) *J. Am. Chem. Soc.* 116, 3097–3101.
53. Fields, B. A., Guss, J. M., and Freeman, H. C. (1991) *J. Mol. Biol.* 222, 1053–1065.
54. Reinhammar, B. R. M. (1972) *Biochim. Biophys. Acta* 275, 245–259.
55. Sykes, A. G. (1991) *Adv. Inorg. Chem.* 36, 377–408.
56. Hall, J. F., Kanbi, L. D., Strange, R. W., and Hasnain, S. S. (1999) *Biochemistry* 38, 12675–12680.
57. Shimidzu, A., Sasaki, T., Kwon, J. H., Odaka, A., Satoh, T., Sakurai, N., Sakurai, T., Yamaguchi, S., and Samejima, T. (1999) *J. Biochem. (Tokyo)* 125, 662–668.
58. Nersissian, A. M., Immoos, C., Hill, M. G., Hart, P. J., Williams, W., Herrmann, R. G., and Valentine, J. S. (1998) *Protein Sci.* 7, 1915–1929.
59. Kataoka, K., Nakai, M., Yamaguchi, K., and Suzuki, S. (1998) *Biochem. Biophys. Res. Commun.* 250, 409–413.
60. Pascher, T., Karlsson, B. G., Nordling, M., Malmström, B. G., and Vänngård, T. (1993) *Eur. J. Biochem.* 212, 289–296.
61. Hall, J. F., Kanbi, L. D., Strange, R. W., and Hasnain, S. S. (1999) *Biochemistry* 38, 12675–12680.
62. Randall, D. W., Gamelin, D. R., LaCroix, L. B., and Solomon, E. I. (2000) *J. Biol. Inorg. Chem.* 5, 16–29.
63. Buning, C., Canters, G. W., Comba, P., Dennison, C., Jeuken, L., Melter, M., and Sanders-Loehr, J. (2000) *J. Am. Chem. Soc.* 122, 204–211.
64. Groeneveld, C. M., Aasa, R., Reinhammar, B., and Canters, G. W. (1987) *J. Inorg. Chem.* 31, 143–154.
65. Coremans, J. W. A., Groenen, E. J. J., Dennison, C., and Canters, G. W., unpublished work.
66. Coremans, J. W. A., Poluektov, O. G., Groenen, E. J. J., Warmerdam, G. C. M., Canters, G. W., Nar, H., and Messerschmidt, A. (1996) *J. Phys. Chem.* 100, 19706–19713.
67. Houtink, C. W. G., and Canters, G. W. (1992) *J. Biol. Chem.* 267, 13836–13842.
68. Bonander, N., Karlsson, B. G., and Vänngård, T. (1996) *Biochemistry* 35, 2429–2436.

BI0006480